LA-UR- 98-2193

Title:

The Influence of Surface Morphology and Oxide Microstructure on the Nucleation and Growth of Uranium Hydride on Alpha Uranium

CONF-981124--

Author(s):
Robert J. Hanrahan
Marilyn E. Hawley
Geoff W. Brown

Submitted to:
Proceedings of MRS Symposium H
"Hydrogen in Metals and Semiconductors"
November, 1998

Los Alamos
NATIONAL LABORATORY

DISCLAIMER

The Influence of Surface Morphology and Oxide Microstructure on the Nucleation and Growth of Uranium Hydride on Alpha Uranium,

R. J. Hanrahan Jr., M. E. Hawley, and G. W. Brown,
Materials Science and Technology Division, Los Alamos National Laboratory, Los Alamos, NM 87545

ABSTRACT

While the bulk kinetics of the uranium-hydrogen reaction are well understood, the mechanisms underlying the initial nucleation of uranium hydride on uranium remain controversial. In this study we have employed environmental cell optical microscopy, Scanning Electron Microscopy (SEM) and Atomic Force Microscopy, (AFM) in an attempt to relate the structure of the surface and the microstructure of the substrate with the susceptibility and site of hydride nucleation. Samples have been investigated with varying grain size, inclusion (carbide) concentration, and thermal history. There is a clear correlation to heat treatment immediately prior to hydrogen exposure. Susceptibility to hydride formation also appears to be related to impurities in the uranium. The oxidized surface is very complex, exhibiting wide variations in thickness and topography between samples, between grains in the same sample, and within individual grains. It is, however, very difficult to relate this fine scale variability to the relatively sparse hydride initiation sites. Therefore, the surface oxide layer itself does not appear to control the sites where hydride attack is initiated, although it must play a role in the induction period prior to hydride initiation.

INTRODUCTION

The kinetics of the uranium-hydrogen reaction have been the subject of many studies and have been well characterized. In the reaction between hydrogen and bulk uranium metal at constant temperature and pressure, para-linear kinetics are observed. The initiation of the reaction has been the subject of some controversy. While early studies identified an "induction period" [1] prior to the reaction initiating, most later studies maintain that this is a product of low gas purity, that in high purity hydrogen the reaction begins immediately.[2] In order for the induction period to be eliminated at temperatures below 100° C it has been shown necessary to sensitize the surface with an anneal at 200-600° C.[3] Most studies have reported that the reaction initiates at discrete sites on the surface of the metal, the number and distribution of which have been observed to vary with surface preparation, grain size, purity, and inclusion size and distribution, among other variables.[4,5,6] The kinetics do vary considerably with the metallurgical condition of the specimen, which effect has been attributed to variations in the nucleation kinetics.[7]

The mechanism of sensitization of the surface has not been identified. Among the previous published studies of the site selection of hydrogen attack on uranium: Owen and Scudmore [4] looked at "pure" U. They identified inclusions (mostly UC) as nucleation sites. They also determined that the nucleation rate decreases as the native oxide film grows. Bloch et al.[6] conducted hydrogen exposures at 1000 torr at 150°-250° C with "pure U" and U-0.1Cr (no analysis). They specifically excluded carbides as nucleation sites, but associated nucleation with random sites in preferential areas such as grain boundaries, slip lines, scratches etc. This study showed extensive attack at all of these sites. A "pitting type" attack was identified as occurring at temperatures below 130° C, by coalescence of several nuclei into a single pit growing into the metal. At higher temperatures the growth appeared to be more of a "lateral spread" type. Moreno et al. [8] investigated U and U-0.1Cr exposed to H at 50° C. They sensitized their samples at 600° C. Very rapid attack was observed at grain boundaries, inclusions, twins etc. They attributed this to transport through the oxide along planar defects formed during oxide growth in the annealing stage.

EXPERIMENTAL

Optical Microscopy

Cylindrical uranium specimens 5 mm diameter, 10mm long, with an 8 mm deep hole drilled in one side for a type K thermocouple were fabricated from uranium stock of 3 different carbon contents, nominally 50, 100, and 300 ppm by weight. In addition to being observed in the as-cast and machined condition, these specimens were subjected to two different thermal treatments involving heating the specimen to the γ phase at 925° C then quenching to less than 100° C in either 10 seconds or 1000 seconds (herein referred to as quenched or slow-cooled) The flat end of the specimens were ground and polished using standard metallographic techniques then electropolished in 5% H_3PO_4 at 4-5 V DC. After polishing the specimens were stored under vacuum. The surface uranium doixide film produced by this treatment was measured using Rutherford Backscattering Spectroscopy. The film thickness was 70 +/- 5 Å with no measurable difference between a fresh surface and one stored in a vacuum dessicator for 48 hours. Additional specimens prepared for AFM were also used for optical microscopy. These were prepared from rolled low carbon (25.73 ppm) uranium sheet 0.5 mm thick. This material was cut into strips 11 mm long by 4 mm wide. Examined in both the as rolled condition and after a γ anneal at 900° C.

For hot stage work, a Leitz vacuum heating stage is mounted on a Zeiss Axiophot microscope with long working distance objectives for magnifications up to 500x. This is connected to a turbo pump station through an entirely stainless steel vacuum system. Prior to introduction into the vacuum system, UHP hydrogen was further purified by passing through an Alfa-Aesar (Pd filter) hydrogen purifier. A digital video camera mounted on the microscope is connected to an image capture board mounted in a personal computer. Images are acquired directly into Image Pro™. Samples were heated to the reaction temperature (70-100° C) in vacuum prior to introduction of hydrogen. Pressure was held nearly constant at 600-650 torr. Pre-annealing varied from no treatment to 30 minutes at 200° C.

Atomic Force Microscopy

AFM studies were performed on rolled foils of low carbon uranium. This material was examined in the as-rolled state and after annealing in the γ phase at 900° C to obtain a strain relieved, equiaxed α uranium microstructure comparable to the cast material. Surface preparation was otherwise the same as described above. Surface morphology was examined in air using AFM data obtained with a Digital Instruments [9] Dimension 3000 scanning probe microscope contained in a glovebox equipped with flowing argon. Imaging was carried out in tapping mode [10] (a non-contact method) with silicon tips on rectangular silicon cantilevers having dimensions 125μm x 30μm x 10μm and ~300 kHz resonant frequency. After electropolishing, each sample was rinsed in methanol and then transferred into the glovebox for initial imaging. After representative areas were scanned, the samples were heated at 200° C for ~10 minutes under an increased Ar flow, and then allowed to cool for one hour. The sample was then scanned again to observe the effect of the heating cycle. Each image was acquired at 512 x 512 resolution. The AFM images were processed by flattening (adjusting the scan line registry for offsets occurring during tip retrace) and background subtraction via plane fit using the Digital Instruments software.

RESULTS

A specimen of uranium (as-cast) containing nominally 100 ppm carbon is shown in figure 1. This specimen was ground, mechanically polished, and electropolished, then exposed to hydrogen at 70° followed by 100° C. While scratches and grain boundaries were clearly preferentially attacked, the overall reaction was slow and relatively uniform. The inclusions (mostly carbides) are the last areas attacked and appear as bright spots on the micrograph. This experiment was repeated with all three different carbon contents and with an additional specimen of very heavily cold worked, fine grained, low carbon (25 ppm C) uranium. In all cases the general result was the same, no pitting of the surface was observed, although three experiments were terminated because the machined sides or edges of the uranium cylinders were preferentially attacked.

Figures 2 shows the surface of a specimen of high carbon (300ppm), slow-cooled uranium which was given a sensitization treatment at 200° C for 10 minutes prior to exposure to hydrogen at 70° C. Almost immediately a few sites began to react, but most of the surface was unaffected. In figure 2, the distortion around the pit caused by the volumetric expansion as the metal is converted to hydride is clearly visible. The pits tended to follow the most heavily distorted regions in the metal as they grew.

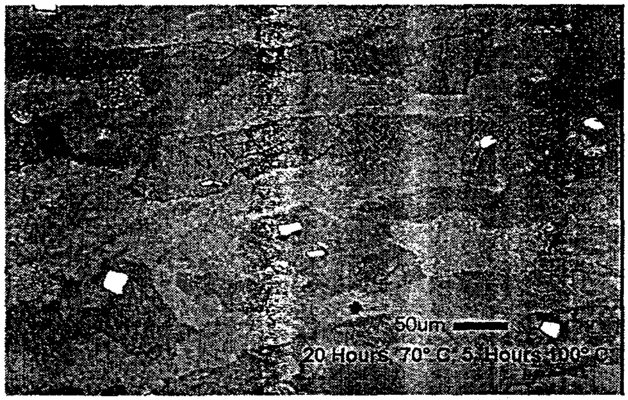

Figure 1. Uranium specimen exposed for 20 hours in pure hydrogen at 70° C, followed by 5 hours at 100° C with no sensitization treatment.

Figure 2. Uranium exposed in pure hydrogen at 70° C after a vacuum anneal at 200° C for 10 minutes.

Figure 3 shows AFM images of an as-rolled foil of low carbon (25 ppm) α-U. Panels **a** and **b** show the same grain before and after heating to 200 °C for 10 minutes under flowing Ar. Panel **c** is the region in the white dashed box of panel **b** and shows an increased density of carbide inclusions in the outlined grain. The inclusions show up as pits after heating, presumably due to growth/roughness increase as the surrounding uranium is oxidized. Panel **d** is a close-up view of regions observed after heating. Based on their morphology these are most likely U(O,C,N) based on uranium oxide.[10] A substructure of hexagonal cracks is observed. . Panels **e** and **f** are from a sample prepared identically. Panel **e** shows the roughness that occurs after heating and panel **f** shows the same area of the sample 24 hours later. A crater has begun to form

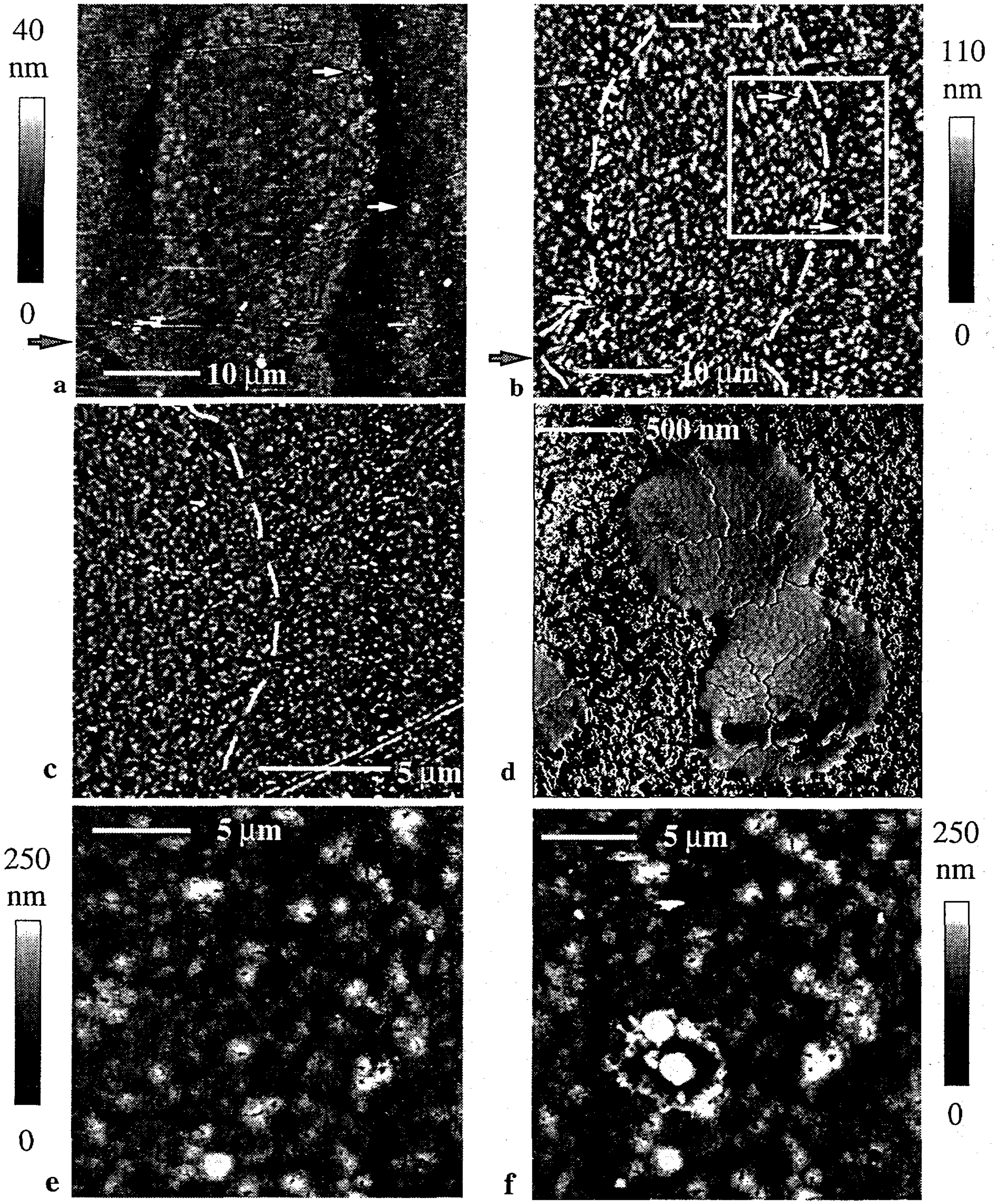

Figure 3. AFM images of rolled α-U. Panels **a** and **b** show the same grain before and after heating to 200 °C for 10 minutes under flowing Ar. Panel **c** is the region in the white box of panel **b** and shows an increased density of carbide inclusions in the outlined grain. Panel **d** is a close-up of a second phase observed after the heating cycle. Cracking occurs coincident with hexagonal substructure. Panels **e** and **f** are from a sample prepared identically. Panel **e** shows the roughness that occurs after heating and panel **f** shows the same area of the sample 24 hours later. A crater has begun to form but no obvious nucleation site is visible in panel **e**. See text for detailed explanation.

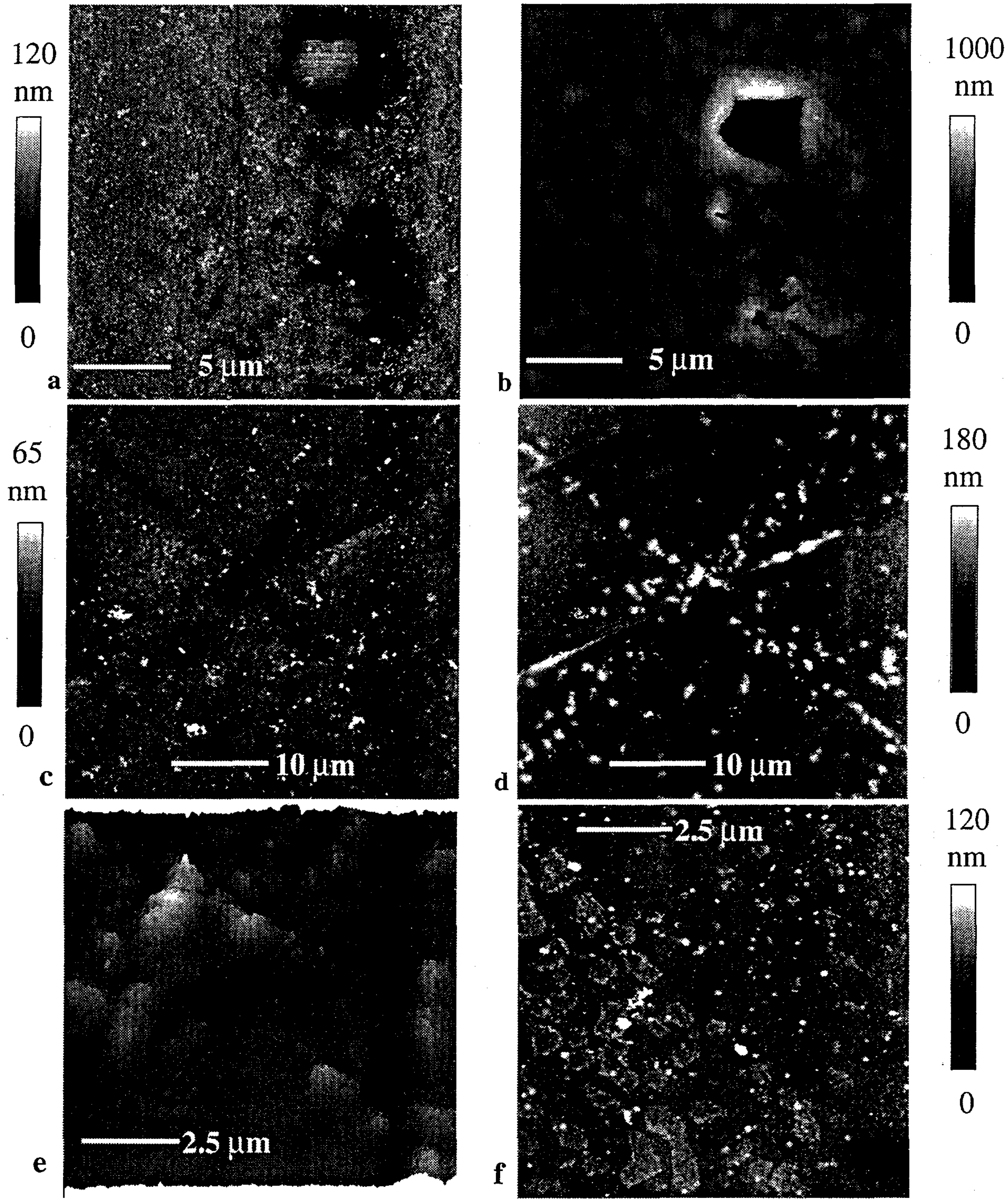

Figure 4. AFM images of the surface of α-U annealed to the γ point in vacuum. Panels **a** and **b** show the area around the same carbide inclusion before and after heating for 10 minutes in Ar at 200 °C, respectively. Enhanced oxidation appears to be occuring around the inclusion. Panels **c** and **d** show a region where twin boundaries and a surface step are visible, again before and after the heating cycle, respectively. Panel **e** is a higher resolution 3-dimensional surface plot of the center of the cross in panel **d**. Panel **f** is taken from a second, identically prepared sample and shows a grain boundary with island-like structures covering the surface of the left grain. See text for detailed explanation.

but no obvious nucleation site is visible in panel **e**. The texture at the edge of the crater is similar to that on the features shown in panel **d.**

Figure 4. shows AFM images of the surface of an α-U foil after annealing in the γ phase at 900° C in vacuum. Panels a and b show the area around the same carbide inclusion before and after heating for 10 minutes in Ar at 200° C respectively. Enhanced oxidation appears to be occurring around the inclusion. Similar behavior is observed around smaller carbide inclusions in other images. Panels c and d show a region on the same sample where twin boundaries and a surface step are visible, again before and after the heating cycle. Preferential oxidation occurs on the twin boundaries and surface step. Panel e is a higher resolution surface plot of the center of the cross in panel d. Panel f is taken from a second, identically prepared sample and shows a close-up of a grain boundary with island like structures covering the surface of the left hand grain.

CONCLUSIONS

At low temperatures, if no sensitization treatment is applied, the hydriding reaction takes a unpredictably long time to initiate and is nearly uniform. Specimens with higher carbon contents appear to be more easily sensitized. A very brief sensitization treatment can result in a very few sites being initiated. These sites can be in otherwise unremarkable areas, away from grain boundaries, near, but not at the edge of inclusions. This observation suggests the possibility that the initiation site is caused by a local chemical inhomogeneity. This is also supported by the enhance oxidation rate observed around carbide inclusions. Otherwise, the oxide surface is highly defective, with obvious changes in roughness and texture along microstructural features, between grains, and within grains. The hypothesis [8] that hydride attack is localized due to structural defects in the oxide resulting from high temperature annealing is very difficult to justify. Our hydriding experiments have shown that this ample supply of local imperfections in the oxide does not correlate with hydride initiation, unless the sample is given a sensitization anneal at a temperature high enough to expect segregation of impurities to the metal surface. Hence, the role of interstitial trace elements which might catalyze the hydriding reaction (F, Cl, S, P,) in the initiation mechanism needs to be explored.

REFERENCES

1) Albrecht, W.M., and Mallet, M.W., J. Electrochem. Soc., **105/10**, 610-11 (1958).
2) Alire, R.M., Mueller, B.A., Peterson, C.L., and Mosley, J.R., J. Chem. Phys., **52,** 37-46, (1970).
3) Bloch J., and Mintz, M.H., J. Less Comm. Met., **166,** 241-51, (1990).
4) Owen, L.W. and Scudmore, R.A., Corr. Sci., **6**, 461-8, (1966).
5) Bloch, J., Swissa, E., and Mintz, M.H., Zeit. Phy. Chem., N. F. **164**, 1193-98, (1989).
6) Bloch, J., Simca, E., Kroup, M., Stern, A., Shmariahu, D., and Mintz, M.H., , J. Less Comm. Met, **103**, 163-71 (1984).
7) Condon, J.B., , J. Phys. Chem, **79/4**, 392-6, (1975).
8) Moreno et al. J. Nuc. Mat. **230**, 181-86 (1996).
9) Digital Instruments, 112 Robin Hill Rd., Santa Barbara, CA, USA 93117
10) A.N. Holden, Physical Metallurgy of Uranium , Addison-Wesley, Reading Massachusetts, 1958. p. 218-23.